

ON THE ORBITAL PERIOD OF THE NEW CATAclySMIC VARIABLE EUVE J2115–586¹

STÉPHANE VENNES

Center for EUV Astrophysics, 2150 Kittredge Street, University of California, Berkeley, California 94720-5030
 Electronic mail: vennes@cea.berkeley.edu

DAYAL T. WICKRAMASINGHE

Department of Mathematics, The Australian National University, Canberra, Australia
 Electronic mail: dayal@mso.anu.edu.au

JOHN R. THORSTENSEN

Department of Physics and Astronomy, Dartmouth College, Hanover, New Hampshire 03755
 Electronic mail: thorsten@dartmouth.edu

DAMIAN J. CHRISTIAN

Center for EUV Astrophysics, 2150 Kittredge Street, University of California, Berkeley, California 94720-5030

MICHAEL S. BESSELL

Mount Stromlo and Siding Spring Observatories, Private Bag, Weston Creek P.O., ACT 2611, Australia
 Electronic mail: bessell@mso.anu.edu.au

Received 1996 June 17; revised 1996 July 24

ABSTRACT

We have obtained phase-resolved spectroscopy (3660–6040 Å) of the recently discovered cataclysmic variable EUVE J2115–586 using the 74-inch telescope at Mount Stromlo Observatory. The radial velocity is modulated over a period of 110.8 min with a possible one-cycle-per-day alias of 102.8 min, and a semiamplitude of $\approx 270 \text{ km s}^{-1}$ at H β and $\approx 390 \text{ km s}^{-1}$ at He II $\lambda 4686$. The spectroscopic appearance (H I Balmer, Ca II, He I, He II emission lines), the orbital period, and the velocity amplitude indicate that this cataclysmic variable is probably an AM Her type; the absence of cyclotron humps indicates a low intensity magnetic field ($B < 20 \text{ MG}$). Extreme ultraviolet emission phased at the orbital period shows evidence of variability, but additional EUV/soft x-ray observations are recommended. © 1996 American Astronomical Society.

1. INTRODUCTION

The number of known magnetic cataclysmic variables (CVs) has recently doubled after completion of the *ROSAT* all-sky survey and ensuing optical identification efforts (see Beuermann & Schwöpe 1994). Recently, Walter *et al.* (1995) and Shafter *et al.* (1995) have identified RX J0515.6+0105 as the longest-period polar ($P = 7^{\text{h}}.98$), although Shafter *et al.* do not rule out a DQ Her classification rather than AM Her. The discovery of several systems (e.g., RX J0531.5–4624, Reinsch *et al.* 1994) in the so-called “period gap” ($2^{\text{h}} < P < 3^{\text{h}}$; see a discussion by Wu *et al.* 1995) was reported, although the statistical significance and viability of this feature in the period distribution is being challenged by recent observations (see Beuermann & Schwöpe 1994) and theory (Wu & Wickramasinghe 1993). At lower energies, extreme ultraviolet (EUV) observations also yield interesting discoveries: Buckley *et al.* (1993) identified RE 1938–461 in the Wide Field Camera survey as one of the first AM Her systems within the period gap; EUVE J1429–380 (Craig

et al. 1996) was discovered during a pointed *Extreme Ultraviolet Explorer* (EUVE) observation (McDonald *et al.* 1994), and Stobie *et al.* (1996) found it to be an eclipsing magnetic CV above the period gap ($P = 4^{\text{h}}.765$). Optical identification programs of faint, yet to be identified EUV sources will certainly uncover several more cataclysmic variables. Population characteristics should then be clarified.

Extreme ultraviolet photometric and spectroscopic observations of magnetic cataclysmic variables provide new insights into the physics of these systems, it is therefore of interest to identify bright EUV sources with magnetic CVs. Spectroscopic observations are currently obtained with EUVE ($E \leq 0.17 \text{ keV}$) at medium resolution ($\lambda/\Delta\lambda \approx 200$). Vennes *et al.* (1995) first reported on the continuum appearance of the spectrum ($75 \leq \lambda \leq 140 \text{ Å}$) of the accretion region on VV Puppis, lending support to the deep heating model of the accretor’s envelope. The source of heating, compression by accretion or hard x-ray radiation, is still unknown. Study of the EUV light curve of UZ Fornacis shows evidence of a vertical extension of the accretion region (Warren *et al.* 1995), possibly caused by thermal expansion or magnetic confinement.

¹Based on observations obtained at Mount Stromlo Observatory.

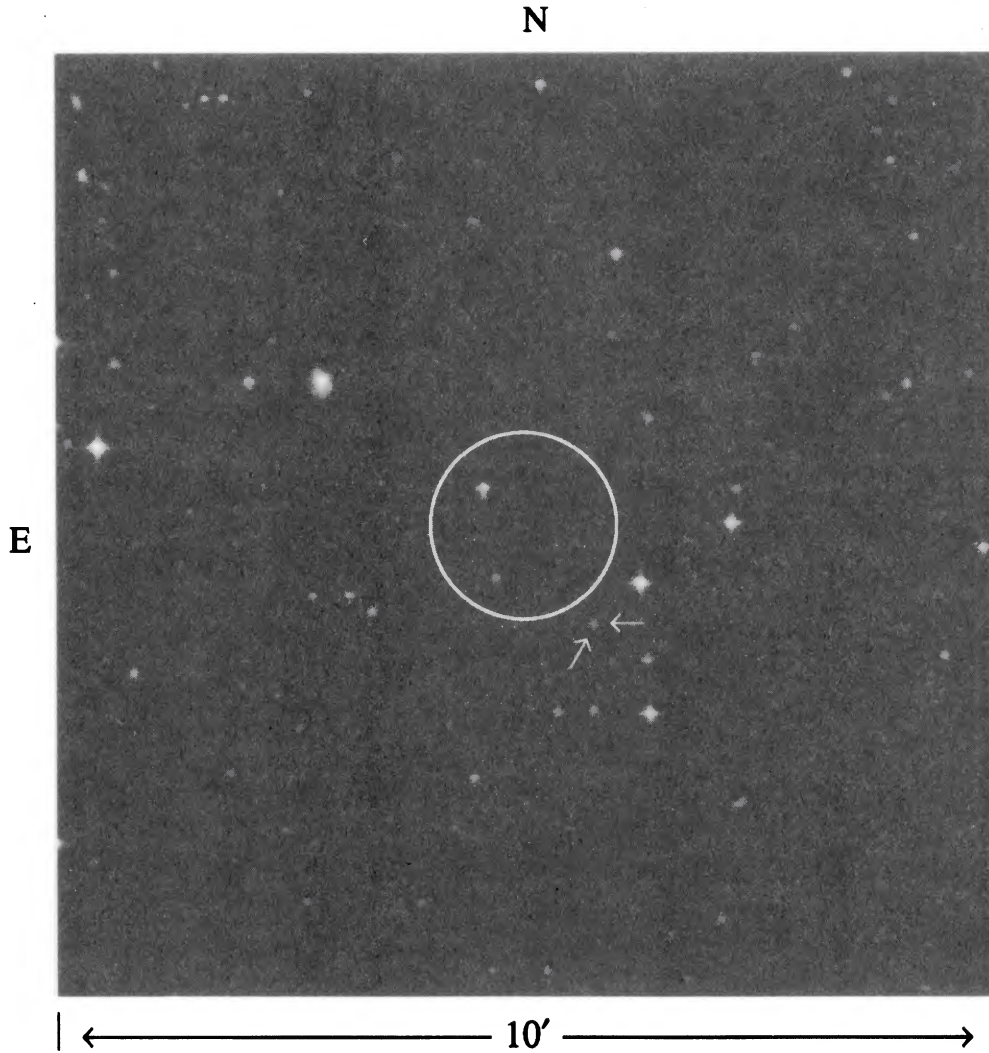


FIG. 1. A $10' \times 10'$ field centered on the EUV source position ($\alpha_{2000}=21^{\text{h}} 15^{\text{m}} 46^{\text{s}}$, $\delta_{2000}=-58^{\circ} 39'8''$). Arrows mark the position of the AM Her-like system EUVE J2115–586 ($\alpha_{2000}=21^{\text{h}} 15^{\text{m}} 41.03^{\text{s}}$, $\delta_{2000}=-58^{\circ} 40' 53''.7$).

EUVE J2115–586 is a faint extreme ultraviolet (EUV) source observed during the *Extreme Ultraviolet Explorer* all-sky survey (Bowyer *et al.* 1994, 1996) from 1992 October 20 to 23 and again from 1993 April 19 to 25. The source was only detected in the shortest-wavelength survey band (100 Å) at a count rate of 0.059 ± 0.012 counts s^{-1} . Following identification of the source with a possible candidate, a new AM Her-like variable (Craig 1996), we have obtained a series of spectra of EUVE J2115–586 at Mount Stromlo Observatory (Sec. 2). Based on these new observations, we constrain the system's orbital period (Sec. 3.1); we present additional properties of the system in Sec. 3.2 and discuss its classification as a probable AM Her in Sec. 4.

2. OPTICAL SPECTROSCOPY

The position of the new cataclysmic variable is marked in Fig. 1 (arrows) along with the error circle centered on the EUV source position (Bowyer *et al.* 1996). We measured the star's coordinates directly from Digitized Sky Survey images using the STSDAS.GASP package and the procedure XYEQ.

We observed EUVE J2115–586 with the 74-inch telescope at Mount Stromlo Observatory on 1996 April 20, 21, 24, and 25 (UT). We used the spectrograph mounted at the Cassegrain focus with a 300 lines mm^{-1} grating and an UVAR thinned Site CCD (1752×532), and we binned the images 2×3 . Because of poor seeing conditions, the slit width was adjusted to 3.0 arcsec except on April 25 when it was reduced to 1.5 arcsec. We obtained exposures of 1200 s on April 20, 600 s on April 21, and 450 s on April 24 and 25. Fe-Ar comparison lamps were obtained after each exposure of EUVE J2115–586; the spectra cover the range from 3660 to 6040 Å at 2.72 Å per pixel, or a 5–6 Å resolution. We obtained continuous two-hour coverage on each of April 21, 24, and 25, but because of mechanical and daylight constraints the hour-angle span of the data set was only 2.4 hours. Figure 2 presents the sum of three spectra obtained on April 20 showing a characteristic AM Her-like emission spectrum; both He II $\lambda 4686$ and H β are broad (FWHM ≈ 15 –20 Å), but He II $\lambda 4686$ is weak indicating a lower state of activity; note the absence of cyclotron humps indicating a low magnetic field ($B < 20$ MG, see Bailey *et al.* 1991).

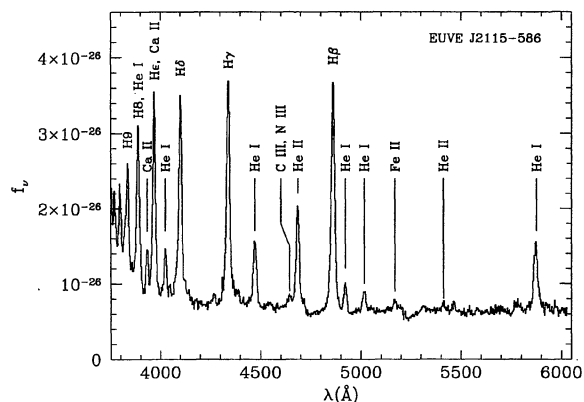


FIG. 2. Blue spectroscopy of the AM Her system EUVE J2115–586. The spectrum is an average of three consecutive 20 min spectra obtained on 1996 April 20. Notable emission features are marked; note the lack of cyclotron emission.

We measured radial velocities using either $H\beta$ $\lambda 4861.33$ or $He II$ $\lambda 4685.68$; a wavelength centroid measurement is obtained by convolution methods using either widely separated “+–” Gaussians (base) or a narrow Gaussian (peak) as the convolution functions (Schneider & Young 1980). The $He II$ $\lambda 4686$ and $H\beta$ peak velocities are optimized for 614 and 676 km s^{-1} FWHM Gaussians, respectively; the widths and separations of the Gaussians for the $He II$ $\lambda 4686$ and $H\beta$ base velocities are 614 and 1750 km s^{-1} , and 676 and 1859 km s^{-1} , respectively. The wavelength scale is well established with the Fe–Ar arc, but errors are introduced by fluctuations of the star’s position within the slit. Monitoring of bright stars reveals systematic errors of $\pm 80 \text{ km s}^{-1}$ with the 3 arcsec slit. We estimate this error at $\pm 40 \text{ km s}^{-1}$ with the 1.5 arcsec slit. Table 1 lists our measurements at 37 epochs (Heliocentric Julian Dates) corresponding to observations obtained on April 20, 21, 24, and 25. Large velocity variations are apparent which is consistent with funnel accretion and offers support to the AM Her classification.

3. ORBITAL PERIOD

3.1 Optical Spectroscopy

We searched for periodicity in the $H\beta$ and $He II$ $\lambda 4686$ emission velocity time series, for both line bases and peaks, by fitting general least-squares sinusoids at trial frequencies separated by $\Delta\nu = (10\Delta T)^{-1}$, where $\Delta T \approx 5^d$ is the span of the data. Figure 3 shows the averaged inverse square residual of all four velocities at each trial frequency (periodogram). As expected from the limited hour-angle coverage, the period is ambiguous; the uncertainty in the cycle count between nightly observations manifests itself as a family of alias frequencies separated by $\Delta\nu = 1 \text{ cycle d}^{-1}$. Frequencies near 13.0 and 14.0 d^{-1} are about equally strong, while others are less so. A Monte Carlo simulation of the measurement (Thorstensen & Freed 1985) showed that given our sampling and noise level, and an orbital frequency similar to the one we find, our data would be expected to select the correct frequency with probability 66%, to make an error of $\pm 1 \text{ d}^{-1}$ with probability 33%, and a $\pm 2 \text{ d}^{-1}$ error with probability

TABLE 1. Radial velocities.

HJD (2450000+)	ν $H\beta$ (base) (km s^{-1})	ν $H\beta$ (peak) (km s^{-1})	ν $He II$ (base) (km s^{-1})	ν $He II$ (peak) (km s^{-1})
194.25059	+135	+100	+228	+185
194.26842	+15	+58	–64	–48
194.28449	–384	–257	–501	–350
195.22830	–199	–238	–229	–243
195.23674	+72	+64	+179	+118
195.24525	+332	+279	+417	+374
195.25457	+351	+333	+348	+363
195.26385	+141	+127	+126	+69
195.27244	+3	+31	–91	–238
195.28161	–126	+20	–291	–272
195.29025	–245	–252	–284	–302
195.29887	–153	–191	–93	–137
195.30760	+4	–22	+136	+99
198.21492	–282	–280	–303	–340
198.22212	–185	–318	–103	–355
198.22877	+39	–84	+247	+164
198.23589	+222	+117	+410	+729
198.24282	+232	+277	+401	+495
198.24967	+136	+100	+283	+322
198.25641	+35	+103	+35	+238
198.26401	–63	+70	–122	–62
198.27131	–159	–100	–275	–171
198.27842	–233	–107	–380	–244
198.28541	–238	–160	–427	–305
198.29262	–307	–311	–252	–355
198.29976	–177	–323	–65	–4
198.30675	+62	–98	+215	+283
198.31445	+213	+428	+429	+598
199.23138	+7	–237	+227	+238
199.23910	+260	–85	+478	+550
199.24700	+364	+189	+379	+208
199.25436	+383	+333	+391	+515
199.26129	+390	+321	+52	+373
199.26845	+196	+158	+94	+194
199.27606	+28	+198	–38	+95
199.28309	–206	–134
199.29019	–410	–241	–531	–454

1%. All four velocity time series independently select either 13 or 14 cycles per day, so we estimate the probability that one of these is correct as $>95\%$. We are somewhat puzzled by the apparent strength of alias periods at $n+0.74 \text{ d}^{-1}$ (where n is integer). These frequencies do appear in artificial data and are understandable as a consequence of the gap in coverage between the first pair of nights and the second pair. However, they are much stronger in the real data than in typical artificial data. To see if one of these frequencies could be correct, we ran a further Monte Carlo simulation testing 12.74 d^{-1} against 13.00 d^{-1} . This gave the incorrect choice only two times in 1000, so unless the noise in the velocities is highly correlated it appears unlikely that the 12.74 d^{-1} alias is correct. However, the strength of the 12.74 d^{-1} family argues against uncorrelated gaussian noise, so the Monte Carlo result may be misleading, and the unlikely possibility that the orbital frequency is $n+0.74 \text{ d}^{-1}$ should be kept in mind.

We adopt a likely orbital period, and a one-cycle-per-day alias:

$$P_{\text{orb}} = 110.75 \pm 0.06 \text{ min, and} \quad (1)$$

$$P_{\text{orb}+1} = 102.83 \pm 0.04 \text{ min.}$$

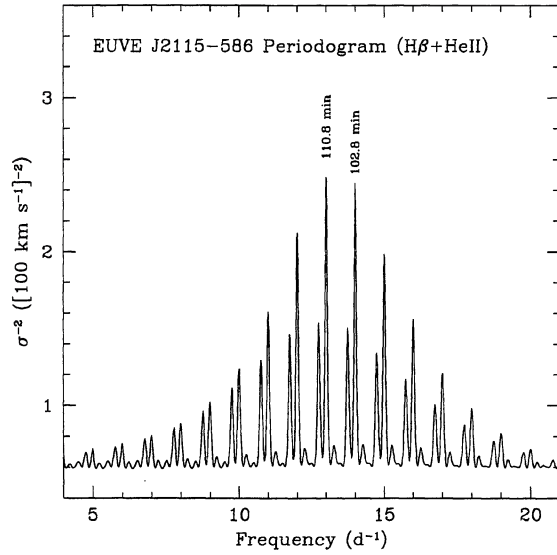


FIG. 3. Summed periodogram of the $H\beta$ and $He\ II\ \lambda 4686$ (base and peak) velocities. The alias periods (110.8 and 102.8 min) are marked.

Additional data, covering a wider hour angle range, should eventually help eliminate the alias period. Results of the period search for individual lines and fitting methods are given in Table 2 for the two possible periods: T_0 corresponds to the conjunction epoch immediately followed with increasing velocity, P is the period, K is the velocity amplitude, γ is the systemic velocity, and σ is the velocity residual relative to the sinusoid fit. Figure 4 shows individual line measurements and sinusoid fits phased with parameters given in Table 2. The scatter considerably exceeds our estimate of the error measurements. In fact, nightly variations in the shape of the velocity curve are perceptible when comparing data taken on 1996 April 21, 24, and 25 (Fig. 5). Moreover, the T_0 epochs show considerable delays between $H\beta$ base and peak measurements, as well as between $H\beta$ and $He\ II\ \lambda 4686$ measurements: the $He\ II\ \lambda 4686$ velocities precede the $H\beta$ veloci-

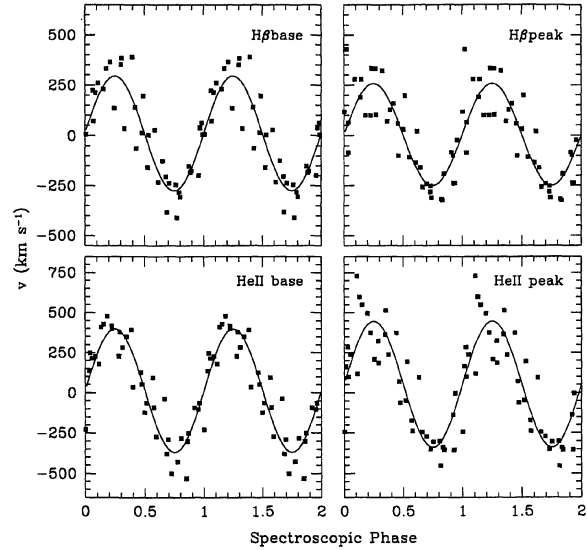


FIG. 4. Velocity measurements based on the $H\beta$ and $He\ II\ \lambda 4686$ lines (base and peak) and phased with the corresponding ephemeris along with best sinusoid fits of the 110.8 min period (see Table 2).

ties by ≈ 0.09 phase while the $H\beta$ peak lags the base by ≈ 0.06 phase. On the other hand, the period measurements are all consistent.

The system appeared to be in a reduced state most of the time: the $He\ II\ \lambda 4686$ line strength is generally weak relative to $H\beta$, and the continuum flux at $5500\ \text{\AA}$ remained constant near $V = 17.4 \pm 0.3$. However, we recorded a steep rise in the $He\ II$ line strength as well as continuum flux, up to $V = 16.2$ from 17.2, on (UT) 1996 April 21 (Fig. 6). The system is, therefore, highly variable and appeared to be only intermittently accreting at that epoch.

3.2 EUV Photometry

EUVE surveyed J2115-586 between (UT) 1992 October 20 and 23, and then again (UT) 1993 April 19 and 25, with

TABLE 2. Orbital properties

	$(P_{\text{orb}} = 110.75\ \text{min})$				
	T_0 (HJD 2450000+)	P (d)	K (km s^{-1})	γ (kms^{-1})	σ (km s^{-1})
$H\beta$ base	198.2309 ± 0.0014	0.07691 ± 0.00006	285 ± 33	10 ± 23	109
$H\beta$ peak	198.2356 ± 0.0017	0.07697 ± 0.00007	254 ± 37	4 ± 26	122
$He\ II\ \lambda 4686$ base	198.2256 ± 0.0011	0.07686 ± 0.00005	384 ± 37	14 ± 26	123
$He\ II\ \lambda 4686$ peak	198.2275 ± 0.0016	0.07691 ± 0.00007	393 ± 53	53 ± 37	173
$\langle P \rangle$...	0.07691 ± 0.00004
	$(P_{\text{orb}+1} = 102.83\ \text{min})$				
	T_0 (HJD 2450000+)	P (d)	K (kms^{-1})	γ (kms^{-1})	σ (km s^{-1})
$H\beta$ base	198.2333 ± 0.0014	0.07141 ± 0.00005	281 ± 34	15 ± 24	113
$H\beta$ peak	198.2378 ± 0.0015	0.07147 ± 0.00006	257 ± 36	11 ± 25	118
$He\ II\ \lambda 4686$ base	198.2283 ± 0.0011	0.07136 ± 0.00004	377 ± 39	15 ± 27	129
$He\ II\ \lambda 4686$ peak	198.2300 ± 0.0015	0.07140 ± 0.00006	390 ± 53	55 ± 37	174
$\langle P \rangle$...	0.07141 ± 0.00003

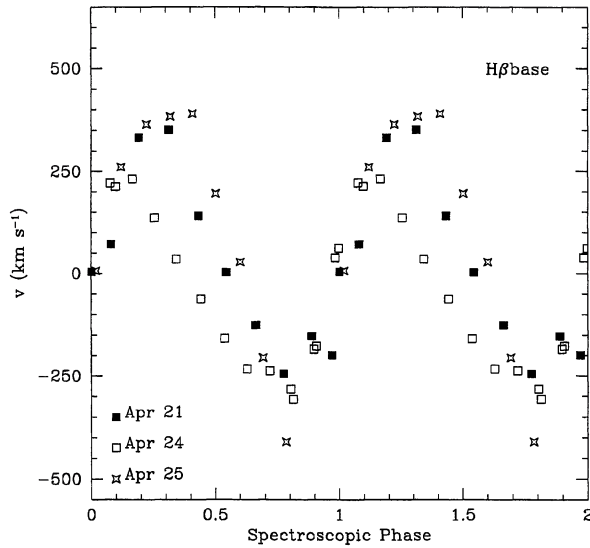


FIG. 5. The $H\beta$ line velocity showing significant nightly variations over the period of 110.8 min. Average orbital properties are derived using the entire set of velocity measurements.

a total exposure of approximately 1200 s. A total of ≈ 40 counts were collected from the source. We generated two lists of events—source and background—using a circular aperture (0.2) centered on the source and an annulus extending to 0.4, respectively. We separately phased all events from the 1992 October observation and from the 1993 April observation using both possible periods ($P=110.8$ or 102.8 min) and arbitrary initial epochs, and redistributed the events in five phase bins. The source appeared marginally variable. We summed the 1992 October and 1993 April data, after arbitrarily phasing the apparent maxima at $\Phi=1.0$. Figure 7

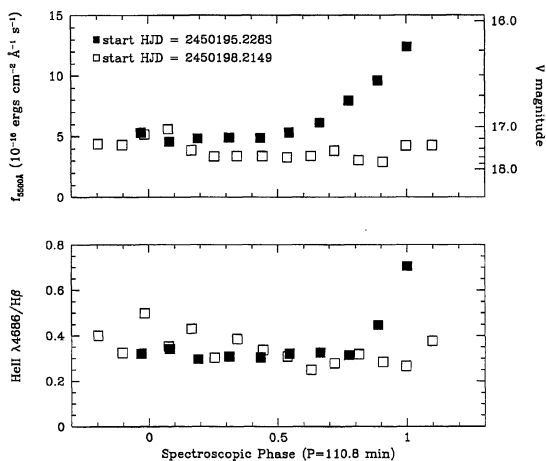


FIG. 6. Monochromatic flux (5500 Å) and line ratio ($\text{He II } \lambda 4686/H\beta$) as a function of phase. The system shows little variability (± 0.3 mag) circa (UT) 1996 April 20–25, but we find evidence of an accretion event on (UT) 1996 April 21. Lack of variability at other times (shown here, 1996 April 24) suggest that the source of accretion was turned off with the exception of intermittent accretion events like this one. Note the simultaneous rise of the $\text{He II } \lambda 4686$ line strength and the continuum flux.

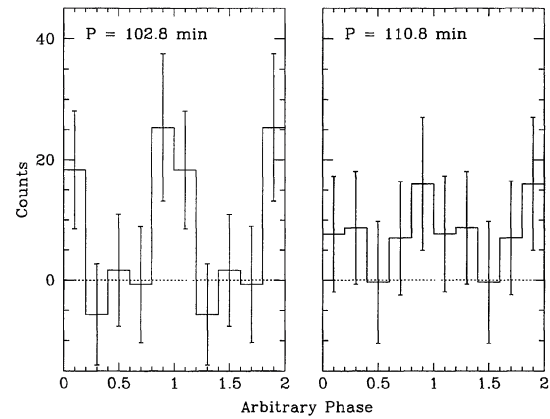


FIG. 7. EUV emission ($EUVE$ 100 Å band) phased with $P=102.8$ and 110.8 min periods. Observed counts are redistributed in five phase bins, and two cycles are shown for clarity. Both light curves show marginal evidence of variability with 3σ ($P=102.8$) and 2σ significance ($P=110.8$).

shows the resulting phased light curves. The 102.8 min period shows an $\approx 3\sigma$ deviation from a constant count rate, while the 110.8 min period shows only an $\approx 2\sigma$ deviation. $EUVE$ pointed observations of sufficient duration would certainly enhance current hints of variability.

4. SUMMARY

We have measured likely orbital periods of the cataclysmic variable $EUVE$ J2115-586: $P=110.8$ or 102.8 min. This system is, therefore, similar to the majority of polars that have orbital periods clustered near 114 min, below the so-called period gap. Radial velocities are characteristic of the accretion stream found in AM Her-like magnetic accretors. The blue spectrum shows no evidence of cyclotron humps, possibly suggesting the presence of a weaker magnetic field ($B \leq 20$ MG); detection of cyclotron emission in red spectra may provide a determination of the magnetic field strength. The system was generally in a reduced state of activity between (UT) 1996 April 20 and 25, except for a sudden rise in activity on April 21. The EUV emission may possibly be variable but additional EUV/soft x-ray observations are necessary to study the energy budget of the accretion region. Circular polarization measurements would firmly establish the association of $EUVE$ J2115-586 with AM Her-like binaries.

This research was supported by NASA Contract No. NAS5-30180 and NASA Grant No. NAG5-2405. The Center for EUV Astrophysics is a division of UC Berkeley's Space Sciences Laboratory. The Digitized Sky Surveys were produced at the Space Telescope Science Institute under U.S. Government Grant No. NAG W-2166. The images of these surveys are based on photographic data obtained using the Oschin Schmidt Telescope on Palomar Mountain and the UK Schmidt Telescope. The plates were processed into the present compressed digital form with the permission of these institutions.

REFERENCES

- Bailey, J., Ferrario, L., & Wickramasinghe, D. T. 1991, *MNRAS*, 251, 37P
Beuermann, K., & Schwope, A. D. 1994, in *Interacting Binary Stars*, ASP Conf. Ser. 56, edited by A. W. Shafter (ASP, San Francisco), p. 119
Bowyer, S., Lampton, M., Lewis, J., Wu, X., Jelinsky, P., & Malina, R. F. 1996, *ApJS*, 102, 129
Bowyer, S., Lieu, R., Lampton, M., Lewis, J., Wu, X., Drake, J. J., & Malina, R. F. 1994, *ApJS*, 93, 569
Buckley, D. A. H., *et al.* 1993, *MNRAS*, 262, 93
Craig, N. 1996, *IAU Circ.*, No. 6297
Craig, N., Howell, S. B., Sirk, M. M., & Malina, R. F. 1996, *ApJ*, 457, L91
McDonald, K., Craig, N., Sirk, M. M., Drake, J. J., Fruscione, A., Vallergera, J. V., & Malina, R. F. 1994, *AJ*, 108, 1843
Reinsch, K., Burwitz, V., Beuermann, K., Schwope, A. D., & Thomas, H.-C. 1994, *A&A*, 291, L27
Schneider, D., & Young, P. 1980, *ApJ*, 238, 946
Shafter, A. W., Reinsch, K., Beuermann, K., Misselt, K. A., Buckley, D. A. H., Burwitz, V., & Schwope, A. D. 1995, *ApJ*, 443, 319
Stobie, R. S., Okeke, P. N., Buckley, D. A. H., & O'Donoghue, D. 1996, *MNRAS*, submitted
Thorstensen, J. R., & Freed, I. W. 1985, *AJ*, 90, 2082
Vennes, S., Szkody, P., Sion, E. M., & Long, K. S. 1995, *ApJ*, 445, 921
Walter, F. M., Wolk, S. J., & Adams, N. R. 1995, *ApJ*, 440, 834
Warren, J. K., Sirk, M., & Vallergera, J. 1995, *ApJ*, 445, 909
Wu, K., & Wickramasinghe, D. T. 1993, *Ann. Israel Phys. Soc.*, 10, 336
Wu, K., Wickramasinghe, D. T., & Li, J. 1995, *PASau*, 12, 165